JOURNAL OF QUATERNARY SCIENCE (2024) 1–13 ISSN 0267-8179. DOI: 10.1002/jqs.3594

JQS Journal of Quaternary Science QRA

The southern Brazilian tropical forest during the penultimate Pleistocene glaciation and its termination

ADRIANA MERCEDES CAMEJO AVILES,[1] MARIE-PIERRE LEDRU,[2]* FRESIA RICARDI-BRANCO,[1] GISELE C. MARQUARDT[3,4] and DENISE DECAMPOS BICUDO[4]

[1]Department of Geology and Natural Resources, University of Campinas, Campinas, SP, Brazil

[2]ISEM, University of Montpellier, CNRS, IRD, Montpellier, France

[3]Departamento de Botânica, Setor de Ciências Biológicas, Centro Politécnico, Universidade Federal do Paraná, Curitiba, Brazil

[4]Instituto de Pesquisas Ambientais, Biodiversity Conservation Dept, São Paulo, SP, Brazil

Received 2 March 2023; Revised 25 October 2023; Accepted 2 January 2024

ABSTRACT: To describe the composition of the penultimate glacial Brazilian Atlantic forest, we analyzed pollen, charcoal and diatoms deposited in the section from 871 to 1400 cm of core CO14 drilled in the Colônia basin in southeastern Brazil. The landscape was characterized by a cool grassland with three conifer genera: *Araucaria*, *Podocarpus* and *Ephedra*. Total arboreal pollen frequency did not change during the transition from glacial to interglacial conditions. Changes in *Podocarpus* frequency and concentration showed out-of-phase responses with austral summer insolation at an orbital scale while, at a millennial scale, both northern and southern hemisphere ice volume controlled the interplay between positions of the Inter-Tropical Convergence Zone and South Tropical Front (STF), which in turn defined the latitudinal distribution of rainfall. The disappearance of *Podocarpus* and the decrease of *Araucaria* observed between ~167 and 160 ka were related to a dry interval which was not observed elsewhere. During Termination II a progressive decrease in conifer pollen taxa was in phase with a southward shift in the STF and increase in Atlantic sea surface temperatures. Our results show that southern hemisphere conifer distribution is strongly linked to austral summer insolation and winter precipitation and will be threatened by the southward expansion of the summer rainfall boundary.

KEYWORDS: *Araucaria*; Atlantic forest; grassland; penultimate glacial; *Podocarpus*

Introduction

On glacial to interglacial time scales, defining the impact of tropical latitudes on high-latitude climates through changes in greenhouse gases is a key to future climate projections (Palaeosens Project Members, 2012). The rate of melting of polar ice and the reorganization of air masses and ocean currents that has taken place in only a few decades challenges all previous millennial- or century-scale scenarios. The last glacial ended with an out-of-phase change in the volume of ice and in the climate in Greenland and in the Antarctic that enhanced a southward shift of the Inter-Tropical Convergence Zone (ITCZ) due to large scale ocean–atmosphere reorganization (e.g. Schneider et al., 2014). Two brief climate reversals, called Heinrich events H1 and H0 (the Younger Dryas) lasting respectively 1000 and 1500 years, were observed within the polar deglaciation, both of which characterized a polar to tropics effect that started in the Northern Hemisphere when the release of sea ice led to wetter climate conditions at the southern edge of the Neotropics (Ledru et al., 2002; Stríkis et al., 2018). Nevertheless, little is still known about the influence of the glacial epochs on the Tropics due to the scarcity of continental tropical records spanning several cold–warm intervals on both orbital and millennial scales. The concentration of deuterium in the Vostok ice core in Antarctica evidenced the redistribution of moisture from the Tropics to the Pole at obliquity scale (Vimeux et al., 2001) and neotropical speleothem records clearly revealed Milankovitch precessional forcing on the monsoon system (Cruz et al., 2005; Burns et al., 2019) related to the expansion of tropical rainforest (Ledru et al., 2009).

The American continent is continuous nearly from pole to pole and thus provides an excellent laboratory for examination of the connections between high and low latitudes in both hemispheres, more specifically the climatic teleconnections in the Southern Hemisphere (Markgraf, 2001; Shulmeister et al., 2006). Since the mid-Pleistocene, the expansion and regression phases of ice volume have been orbitally paced by a 100 000-year cycle that, in turn, has affected the tropical hydrological cycle in the high Andes (Hanselman et al., 2011; Torres et al., 2013; Rodbell et al., 2022) as well as in the lowlands (Kern et al., 2023). However, differences in the expression of the glacial epochs and more particularly between the last glacial, Marine Isotopic Stage (MIS) 2–4, and the penultimate glacial, MIS 6, suggest the influence of other forcings on climate and vegetation at millennial scale (Zheng et al., 2013). Continuous melting of ice and smooth transition phases during MIS 6 suggest a more stable ice cover and less climate variability with lower temperatures than in the last glacial (Obrochta et al., 2014). MIS 6 was characterized by lower temperatures than the last glacial at Lake Titicaca in the high Andes (Hanselman et al., 2011) and in Australasian forests (Kershaw et al., 2007; Ryan et al., 2012). The high-resolution pollen record of Fuquene in the Colombian Andes revealed several shifts in the upper forest limit during MIS 6 that were attributed to short-term climate cycles (Bogotá et al., 2016) that

*Correspondence: Marie-Pierre Ledru, as above.
Email: marie-pierre.ledru@ird.fr

are also clearly visible in a Peruvian speleothem (Burns et al., 2019). However, these millennial-scale events in MIS 6 were of lower amplitude and intensity than those in the last glacial. In the Southern Hemisphere, they are associated with an increase in monsoon activity related to shifts in the ITCZ (Bogotá et al., 2016; Burns et al., 2019). In addition, a strong teleconnection between the eastern Atlantic Ocean and the Agulhas leakage (Caley et al., 2012; Hou et al., 2020) forced the accumulation of warm waters in the southern Atlantic Ocean inducing out-of-phase sea surface temperature (SST) minima with the Northern Hemisphere (Santos et al., 2017). In the southwestern Atlantic Ocean (24°S), MIS 6 is divided into three sub-intervals with marked SST variability between 185 and 160 ka (Santos et al., 2017) in agreement with the Peruvian speleothem record (Burns et al., 2019). However, marine records in the southern Pacific showed that the amplitude and strength of the climatic signal during the glacials was differently expressed depending on the latitude and position of the sub-tropical front (Pahnke et al., 2003).

Multi-proxy analyses of sediment cores collected in the Colônia basin in southeastern Brazil revealed the importance of monsoon activity in driving floristic changes of the Atlantic rainforest during the last glacial (Ledru et al., 2009; Rodríguez-Zorro et al., 2020). Here, to evaluate how changes in ice volume affected the floristic composition of a southern tropical forest, we performed a high-resolution pollen and diatom analysis of a section of core CO14 that covers the penultimate glacial and the transition to the last interglacial [Termination II (TII)].

Study area

The Colônia basin is a circular structure with a diameter of 3.6 km located in the district of Parelheiros, south of the city of São Paulo, in Brazil (23°52′03″S, 46°42′27″W) (Figure 1) (Riccomini et al., 1991, 2011). Topographical relief is relatively low with elevations ranging between 715 and 900 m asl and there is a circular ridge rising to ~125 m above the bottom of the basin (Riccomini et al., 1991, 2011). The age of the structure is estimated at between 11.2 and 5.3 Ma (Simon et al., 2020). A seismic survey revealed organic-rich sediments deposited above a layer of rocks at a depth of ~450 m (Prado et al., 2019).

Mean annual precipitation at Parelheiros is 1600 mm, with a 2-month dry season in July and August. Mean annual temperature is 20°C, with a mean of ~17°C in winter (INMET, 2019; DAEE, 2020; Rodríguez-Zorro et al., 2020). A small river, the Vargem Grande, runs through the basin exiting through a single outlet in the eastern ridge of the structure (Riccomini et al., 2011). Modern climate conditions at Colônia show that an increase/decrease in moisture is driven by changes in the amplitude and intensity of the summer monsoon associated with a southward/northward shift of the convergence zones (ITCZ and South Atlantic Convergence Zone) (Marengo et al., 2020). Farther south, between 27 and 35°S, in southern and southwestern Brazil, the climate shows a gradual change in the peak wet season from austral summer to spring and late winter while in the southeastern region of southern Brazil the peak wet season is observed during austral winter, a climate pattern characteristic of cold air penetration associated with extratropical moisture. Today, the influence of the South American Summer Monsoon (SASM) is observed on the coast until 25°S (Grimm et al., 2000; Orrison et al., 2022).

The circular ridge that surrounds the Colônia basin (Ledru et al., 2015) forms a barrier that prevents any upward deposition of pollen originating from the coastal lowlands. Today vegetation is characterized by a mixed ombrophilous forest in the Atlantic forest domain. Botanical surveys in the basin showed that Myrtaceae, Melastomataceae, Arecaceae and Cyatheaceae are the dominant families with an importance value index of 60%. The most common species include *Myrceugenia campestris* (DC.) D.Legrand & Kause, *Psidium cattleianum* Sabine, *Myrcia tomentosa* (Aubl.) DC. (Myrtaceae), *Tibouchina mutabilis* (Vell.) Triana (Melastomataceae), *Cyathea atrovirens* (Langsd. & Fisch.) Domin (Cyatheaceae), *Symplocos* aff. *celastrinea* Mart. (Symplocaceae) and *Daphnopsis fasciculata* (Meisn.) Nevling (Thymeleaceae) (Marçon, 2009).

Surface pollen samples collected in 2001 in the middle of the basin showed 40% arboreal pollen (AP) with: *Podocarpus* 0.7%, *Alchornea* 2%, Arecaceae 2%, Ericaceae 1%, *Ilex* 1.5%, *Myrsine* 2.5%, Myrtaceae 6%, Melastomataceae–Combretaceae 21%, *Symplocos* 1%, *Weinmannia* 6%, Poaceae 5.5% and Asteraceae tubuliflorae 9.5% (Ledru et al., 2009; Montade et al., 2019). In 2014, a *Weinmannia* treelet was observed in the center of the basin near the coring site. Today, a few *Podocarpus sellowii* Klotzsch ex Endl. trees grow at the state park 'Serra do Mar' near Colônia, in open vegetation at ~850 m asl, which is a low elevation compared to that of other Brazilian altitudinal grasslands (Garcia & Pirani, 2003, 2005; Scheer & Mocochinski, 2016).

Methods and material

Coring and lithology

In 2014, a 1400-cm sediment core (CO14) was collected from a swamp located in the Colônia basin using a D-section Russian corer. The core reached a depth of 14 m and is described in Ledru et al. (2015). Between a depth of 14 and 9 m, the sediments are silt–clay, with compacted organic peat containing plant fibers in the top 9 m of the core. The core is stored in a cold chamber at ISEM-Montpellier, France.

Chronology and geochemical analyses

The chronological framework of core CO14 spans a period of 180 ka based on 22 radiocarbon dates, optically stimulated luminescence (OSL) and paleomagnetism, and the mean annual air temperature (MAAT) curve was fitted to the benthic $\delta^{18}O$ LR04 stack using three changes in temperature as tie points (see details in Rodríguez-Zorro et al., 2020).

Details on X-ray fluorescence (XRF) analyses, mean annual air temperature (MAAT) based on the analysis of branched glycerol dialkyl glycerol tetraethers (brGDGTs) performed on 92 samples, and microcharcoal analyses are given in Rodríguez-Zorro et al. (2020).

Pollen and diatom analyses

A total of 264 pollen samples were collected at 2-cm intervals from the bottom section of core CO14, between 1400 and 871 cm. The pollen samples were prepared using a 0.5 cm^3 sample volume and two tablets of *Lycopodium clavatum* L ($n = 3862$, 9666 ± 671 spores per tablet), and treated with 40% HF, 15% HCl, 10% KOH and density flotation $ZnCl_2$ using the protocol established by Faegri & Iversen (1989). Pollen and spore residues were mounted in glycerol for microscope analysis. Pollen counts reached a total of at least 300 terrestrial pollen grains, not including aquatic, water-level-related taxa or spores. Pollen and spores were identified based on published atlases (Lorscheitter et al., 1998, 1999; Colinvaux et al., 1999; Leal et al., 2011; Lorente et al., 2017), and the pollen reference collection of the Geosciences Institute at the Universidade Estadual de Campinas (UNICAMP) (Fernandez et al., 2021). The pollen taxa and

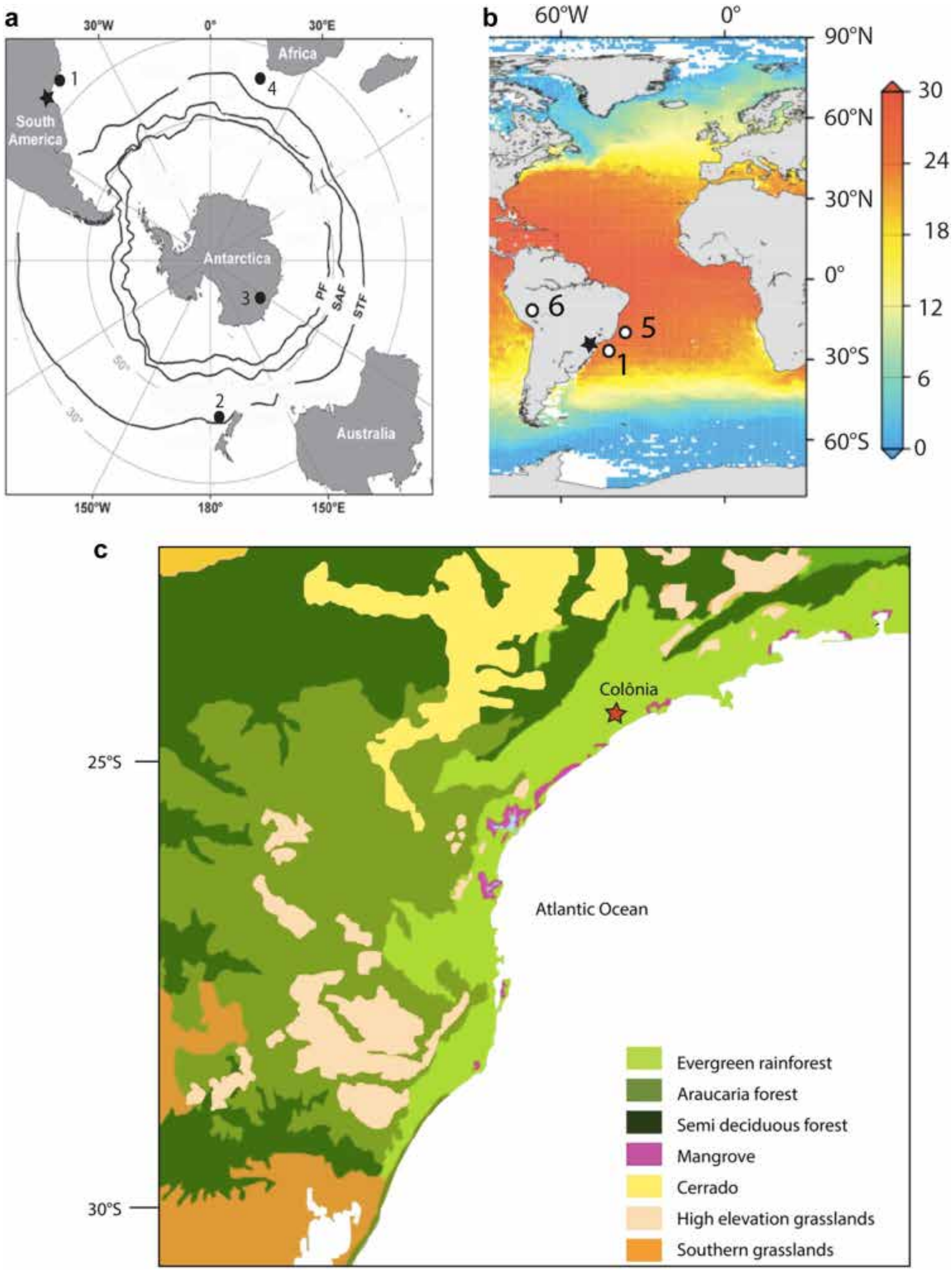

Figure 1. (a) Map of the Southern Hemisphere showing the location of the Colônia basin (red star) and the sites mentioned in the text: (1) core GL-1090 (Santos et al., 2017), (2) core MD97-2120 (Pahnke & Zahn 2005), (3) Epica Dome C (Jouzel et al., 2007), (4) core ODP 1090 (Martínez-Garcia et al., 2010) and the present-day position of the polar front (PF), the sub-Antarctic front (SAF) and the sub-tropical front (STF). (b) Map of South America showing the location of the sites mentioned in the text: (5) Huagapo Cave (Burns et al., 2019), and (6) cores M125-55-7 and M125-55-8 (Hou et al., 2020) represented on austral winter (July to September) average seasonal sea surface temperatures (color shading) (from World Ocean Atlas, 2018). (c) Vegetation types in the region of Colônia; the red dot shows the location of Colônia (from Olson et al., 2001). [Color figure can be viewed at wileyonlinelibrary.com]

their associated ecological assignments are described in Camejo et al. (2022). The pollen diagram and the stratigraphically constrained classification of spectra (CONISS) were generated in Psimpoll (Bennett, 1996, 2009).

Thirty-two 0.5-cm^3 subsamples taken at ~10-cm intervals were prepared for diatom analysis following the procedure described by Battarbee (1986), using heated 30% hydrogen peroxide (H_2O_2) and 37% HCl to remove organic matter. Permanent slides were mounted in Naphrax (RI = 1.74). Diatoms were counted and identified at a magnification of 1000×. A minimum of 400 valves were counted per slide (Battarbee et al., 2001) at an efficiency count of at least 90% (Pappas & Stoermer, 1996). Species abundances are expressed as percentages of the total diatom counts in each subsample. Diatom frustules were identified to the species level whenever possible, and grouped according to their life form (habitat). The ratio of plankton to benthic diatoms (P/B ratio) was used as a proxy for lake level, although it is known to indicate trophic changes mainly in disturbed environments (Fontana et al., 2014). Biostratigraphic diagrams were produced using R 3.1.3 (R Core Team 2022) and the 'vegan' (Oksanen et al., 2019) and 'Rioja' (Juggins 2017) packages. Only taxa showing relative abundances ≥2% are illustrated.

Results

Our section of the core representing a depth of 1400–871 cm is dated to between 181 and 128 ka, thus almost covering MIS 6 and TII between 135 and 128 ka. Sample resolution is 100

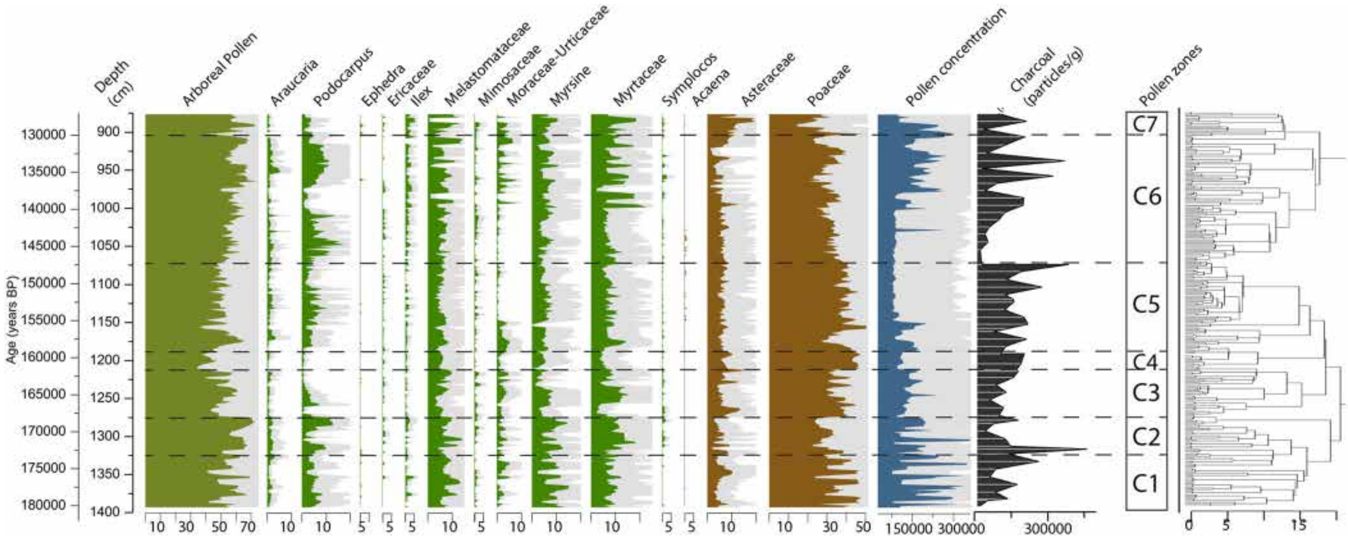

Figure 2. Summary pollen diagram showing arboreal pollen and frequencies of 14 selected taxa and microcharcoal concentration through time. The parts shaded in gray represent the 4× exaggeration curves. The dashed horizontal lines represent the pollen zone boundaries. [Color figure can be viewed at wileyonlinelibrary.com]

years per sample and the time interval between two samples is ~100 years.

Diatoms

The diatom analyses showed two contrasting sections (Figure 3; Supporting Information Fig. S1); the lacustrine part of core CO14 with 12 samples containing diatoms dated between 180 and 153 ka, and a section lacking diatoms from 151 to 128 ka, in agreement with the disappearance of the lacustrine sediment. Thirty diatom species were identified in the bottom part of core CO14. Although the diatom assemblage is dominated primarily by *Pseudostaurosira crateri* Marquardt & C.E. Wetzel, a benthic (pennate) taxon, it is composed mostly of unknown species (Marquardt et al., 2021a, 2021b) and ecological interpretations were based on modern 'analog' species and modern ecological information (Bradbury et al., 1994; Mackay et al., 2005).

Pollen analyses

Pollen content

A total of 132 taxa were identified (Fig. S2a–d) representing 72 plant families, one alga, 10 ferns, three gymnosperms and 58 angiosperms. The 14 pollen taxa shown in the summary diagrams (Figure 2 and S3) were selected based on their proportion in the pollen counts and their ecological significance as defined in modern pollen rain studies (Montade et al., 2019; Portes et al., 2020) and botanical surveys (Garcia & Pirani, 2005; Marçon, 2009; Garcia et al., 2014; Scheer & Mocochinski, 2016). Gymnosperms are represented by three genera, *Araucaria*, *Podocarpus* and *Ephedra*, all associated with low temperatures. *Podocarpus* and *Araucaria* are generally associated with cold and wet climate conditions (Quiroga et al., 2016) while *Ephedra* is associated with cold and dry conditions (Marchant et al., 2002). *Araucaria* requires a minimum of 1400 mm mean annual precipitation and mean annual temperatures below 18°C and below 10°C in winter (Backes, 2009). The plant assemblage Poaceae, Asteraceae and *Myrsine* characterizes high-elevation grasslands (Portes et al., 2020; Safford, 2007). The taxon *Acaena*/*Polylepis* represents the herb *Acaena* and the tree *Polylepis*. *Polylepis* is strictly restricted to the Andes at elevations between 1800 and 3500 m asl (Kessler, 1955) and has never been recorded in modern vegetation in southern Brazil. *Acaena* is mainly observed in high-elevation grasslands with two species recorded in the State of São Paulo, *Acaena eupatoria* Cham. & Schltdl. and *Acaena fruscescens* Bitter (Flora do Brasil, 2022). Thus, the *Acaena/Polylepis* pollen type was attributed to *Acaena* and associated with cold and dry climate conditions. *Acaena* is a low pollen producer with short-distance dispersal (Salgado-Labouriau, 1979). *Ephedra* is restricted to the southernmost region of Brazil and farther south (Flora do Brasil, 2022). Tree ferns of the Atlantic forest, *Dicksonia*, *Lophosoria* (Dicksoniaceae) and *Cyathea* (Cyatheaceae), are associated with moist regional climatic conditions (Montade et al., 2019).

Taxa related to edaphic water levels, *Echinodorus*, Cyperaceae, *Eriocaulon*, *Juncus* and *Utricularia*, characterize bog habitats while the aquatic taxon *Myriophyllum*, the lycophyte *Isoetes* and the alga *Botryococcus* are associated with a shallow lake.

Pollen zones

Pollen grains are well preserved with concentrations ranging between 359 253 and 55 209 grains cm^{-3}. The definition of the seven pollen zones (C1 to C7) was based on changes in AP and non-arboreal pollen (NAP) frequencies and CONISS groupings (Figure 2). The diatom analyses are detailed in Fig. S1.

Zone C1 (1400–1326 cm, ~181–174 ka, 39 samples)

Zone C1 is characterized by a mean concentration of 177 771 pollen grains cm^{-3} (range 352 809–55 209). AP ranged between 41% and 69% with *Araucaria* (0–3%) and *Podocarpus* (2–10%) A peak in *Araucaria* of 3% occurred at 175 ka. Other tree pollen taxa present are *Myrsine* (2–15%), Myrtaceae (5–12%), Moraceae/Urticaceae (0–5%), *Ilex* (0–4%) and Melastomataceae (5–14%); NAP was dominated by Poaceae (23–48%) and Asteraceae (2–9%). In this zone, both *Acaena* and *Ephedra* (0–1%) are present at ~179 ka. Diatoms are represented by 10% planktonic species between 180 and 179 ka, mainly *Aulacoseira ambigua* (Grunow) Simonsen (0–15%), and 90% benthonic species, the most diverse of the record, mainly *Pseudostaurosira crateri* Almeida (18–64%) and *Staurosirella* aff. *leptostauron* var. *dubia* (Grunow) Edlund (12–18%).

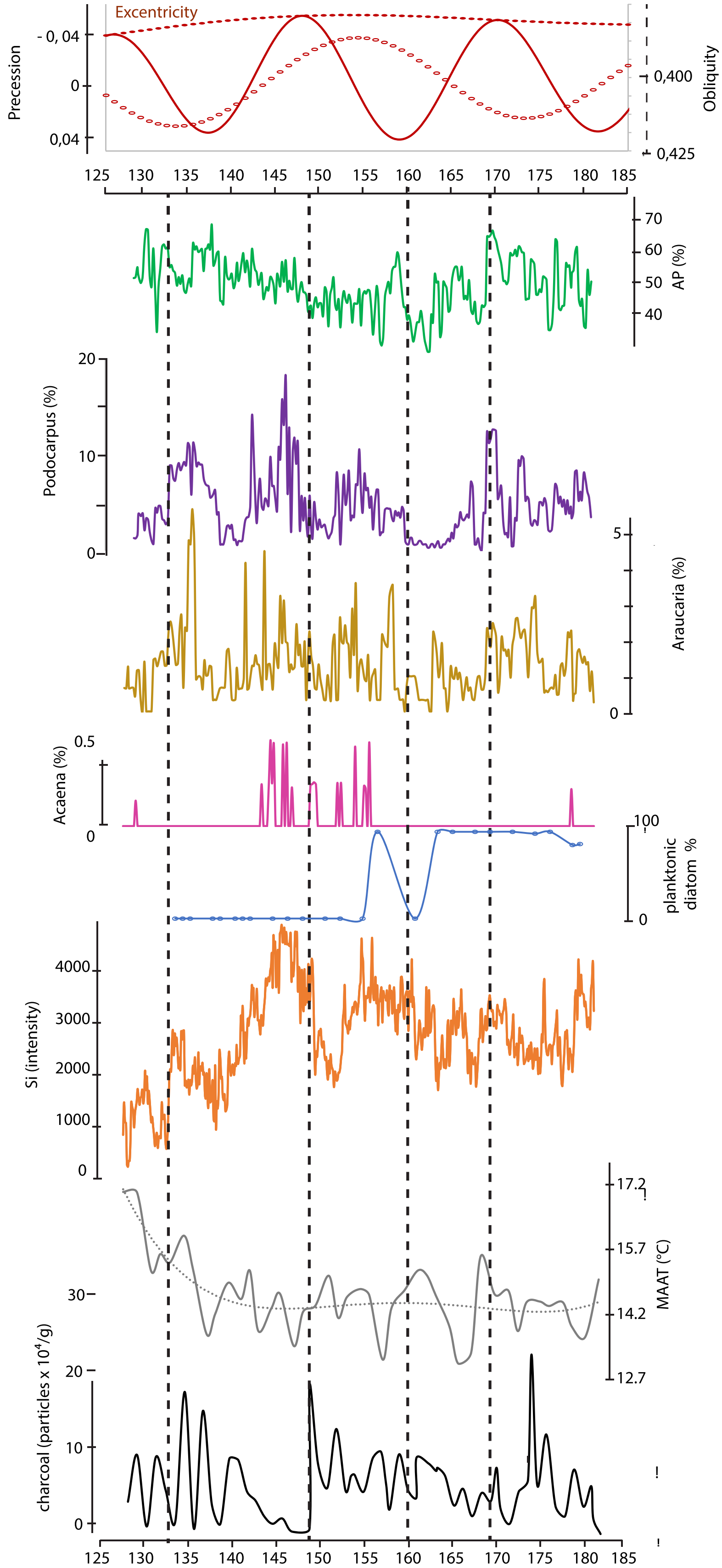

Figure 3. Paleoecological changes in section 871–1400 cm of core CO14 represented by: MAAT (°C), Si intensity and microcharcoal particles (from Rodríguez-Zorro et al., 2020); and the frequency of arboreal pollen of *Araucaria, Podocarpus* and *Acaena/Polylepis* pollen (this study). Orbital cycles represent changes in insolation at 23°S latitude (Laskar et al., 2004). The vertical dashed lines show the changes in vegetation discussed in the text. [Color figure can be viewed at wileyonlinelibrary.com]

Zone C2 (1324–1282 cm, ~174–170 ka, 22 samples)

This zone is characterized by the highest pollen concentration of the whole record: between 359 253 and 62 693 grains g^{-1} with the maximum at ~172 ka and the highest AP frequencies between 50% and 73%. Tree taxa are represented by *Araucaria* (1–3%) and *Podocarpus* (0–13%), Myrtaceae (6–18%), *Myrsine* (4–15%), Moraceae/Urticaceae (0–5%), *Ilex* (0–2%), Ericaceae (0–1%) and Melastomataceae (4–14%). Among the NAP, Poaceae (23–41%) and Asteraceae (2–9%) are best represented.

Ephedra is also present (0–0.3%). Diatoms are 100% benthonic, with *Pseudostaurosira crateri* Almeida (38%) and *Staurosirella* aff. *leptostauron* var. *dubia* (Grunow) Edlund (26%).

Zone C3 (1280–1218 cm, ~170–162 ka, 32 samples)

Zone C3 is characterized by a decrease in pollen concentration (from 249 982 to 73 032 grains g^{-1} and in AP frequency (62–38%): *Araucaria* (0–2%), *Podocarpus* (0–7%), Myrtaceae (2–16%), *Myrsine* (0–9%), Moraceae/Urticaceae (0–6%), *Ilex* (0–1%), Ericaceae (0–1%) and Melastomataceae (3–10%). NAP is characterized by Poaceae (28–47%) and Asteraceae (4–11%). Diatoms are represented by the same benthonic taxa as in the previous zone.

Zone C4 (1216–1188 cm; ~162–160 ka, 15 samples)

This zone is characterized by a mean pollen concentration of 110 618 (range 155 164–81 789) grains g^{-1} with AP frequency the lowest of the record (40–53%). Individual taxon frequencies include *Araucaria* (0–1%), *Podocarpus* (0–5%), Myrtaceae (4–12%), *Myrsine* (0–7%), Moraceae/Urticaceae (0–5%), *Ilex* (0–1%), Ericaceae (0–1%) and Melastomataceae (3–7%). NAP frequencies are represented by Poaceae (39–47%) and Asteraceae (5–9%). Diatoms are 100% benthonic, with *Pseudostaurosira crateri* (38%) and *Staurosirella* aff. *leptostauron* var. *dubia* (37%).

Zone C5 (1186–1071 cm, ~160–148 ka, 57 samples)

The mean pollen concentration in zone C5 is 79 440 grains g^{-1} (189 758–66,135) with an increase in AP frequency (36 to 67%): *Araucaria* (0.3–3.5%) and *Podocarpus* (0.6–10%), Myrtaceae (5–14%), *Myrsine* (0–9%), Moraceae/Urticaceae (decreasing from 4–5% at the beginning of the zone to 0–1% at the end of the zone), *Ilex* (0–1.5%) and Melastomataceae (2.5–8%). Major NAP taxa are Poaceae (28–51%) and Asteraceae (4–8%). Diatoms are represented by benthonic taxa, *Pseudostaurosira crateri* (21%), *Staurosirella* aff. *leptostauron* var. *dubia* (4%) and *Gomphonema* aff. *gibberum* (66%).

Zone C6 (1071–907 cm, 148-132 ka, 79 samples)

Zone C6 is characterized by a decrease in pollen concentration between 261 402 and 59 769 grains g^{-1}, a decrease in AP frequency (49–68%): *Araucaria* (0.3–5.5%), *Podocarpus* (0.6–18%), Myrtaceae (4–22%), *Myrsine* (2–11%), Moraceae/ Urticaceae (0–8%), *Ilex* (0–3%), Ericaceae (0–1%) and Melastomataceae (1–13%). NAP taxa include Poaceae (21–40%) and Asteraceae (1–13%). *Acaena* (0–0.6%) is present with maximum frequencies at ~145 ka. Diatoms are represented by 100% benthonic taxa, mainly *Pseudostaurosira crateri* (50%) and *Staurosirella* aff. *leptostauron* var. *dubia* (12%).

Zone C7 (907–871 cm, 132–128 ka, 18 samples)

Zone C7 is characterized by an increase in pollen concentration to 160 307 grains g^{-1} (75 840–296 671), and an increase in AP frequency (40%–72%) with *Araucaria* (0–1.5%), *Podocarpus* (0.6–4.6%), Myrtaceae (6–18%), *Myrsine* (3–10%), Moraceae/Urticaceae (0–6%), *Ilex* (0–5%) and Melastomataceae (0.6–14%). NAP taxa include Poaceae (14–49%), Asteraceae (5–19%) and *Acaena* (0–0.2%). No diatoms were observed.

Discussion

Change from a lake to a peat bog

Interpretation of the diatoms revealed a significant change in the basin with the progressive evolution from a permanent shallow lake in the penultimate glacial to the formation of a peat bog and the disappearance of the lake at the beginning of the last interglacial (Figure 3 and S1). A dominance of araphid species until 160 ka is consistent with shallow-water conditions (Davydova et al., 2001). Small-celled fragilarioid diatoms are common in depleted nutrient and mineral environments (ombrotrophic conditions), as long as there is enough moisture to survive (Rühland et al., 2009; Hargan et al., 2015). During this low lake period detrital deposition was high (see Si on Figure 3). The associated benthic assemblage suggests that the margins of the lake were colonized by acidophilous and epiphytic taxa, mainly *Pinnularia* and *Eunotia* (Hargan et al., 2015; Costa et al., 2017; Paull et al., 2017), indicating oligotrophic (oligotrophic–dystrophic) environments. In addition, the presence of benthic diatom assemblages reflects circumneutral to slightly acidic conditions in the lake (Metzeltin & Lange-Bertalot, 1998; Krammer, 2000; Unkel et al., 2010) and swamp and peat bog formation around the lake (Sterken et al., 2008) with increased turbidity and more particulate matter. The following increase in the epiphytic and acidophilous taxon *Gomphonema* (Fig. S1) was probably caused by a reduction in light availability beneath the plants when the lake was colonized and gradually became shallower, suggesting a well-developed aquatic vegetation with a small peak in plankton species representing the peat–lake interface. *Aulacoseira ambigua* is commonly found in lotic and lentic environments in different regions in Brazil (Tremarin et al., 2013; Bicudo et al., 2016) and usually observed in relatively cold (~19.3°C), slightly acid (pH 6) and mesotrophic waters of reservoirs (Bicudo et al., 2016). Finally, the shallow lake was replaced by a swamp. The organic matter derived from the plants mentioned above accumulated in the lake sediment and could be associated with the drop in lake level. A sterile zone with no diatoms is observed at this stage. A plausible hypothesis to explain poor diatom preservation at Colônia is dissolution caused by an undersaturated silica environment and organic acids existing under oxic conditions (Bennett et al., 1991; Gell et al., 1994). This conclusion is corroborated by the parallel mass expansion of *Botryococcus* (Fig. S2d). *Botryococcus pila* J.Komárek & P.Marvan characterizes the dystrophic water of small peaty lakes and its high frequency is probably associated with the poor preservation of diatoms, as the oil compounds stored by these algae break up and produce organic acids during decay, which, in turn, triggers the dissolution of siliceous compounds (Komárek & Jankovská, 2001). Finally, the dominance of *Botryococcus* algae suggests that competition between species was low during its deposition (Tyson 1995), which may have resulted from the lack of nutrients in the environment (Tyson 1995).

Vegetation at Colônia during the penultimate glacial

Two taxa associated with cold and dry climate conditions, *Ephedra* and *Acaena*, are no longer observed in the vegetation today (Garcia & Pirani, 2005; Camejo et al., 2022). Two rare taxa are observed today as single isolated trees: *Araucaria* grows inside the basin and is linked to low temperatures and high moisture levels, and *Podocarpus* with *P. sellowii* found in the high-elevation grassland of the state park 'Serra do Mar' near Colônia (Garcia & Pirani, 2005). Two species of *Podocarpus*, *P. sellowii* and *P. lambertii* Klotzsch ex Endl., are observed today in southern Brazil associated with *Araucaria*, either in high-elevation grassland (*P. sellowii*) or in the shade provided by the *Araucaria* forest (*P. lambertii*). *P. sellowii* is always observed in riverine or swamp forests where soil moisture content is higher than in the grassland (Ledru et al., 2007; Teixeira & Assis, 2011). Thus, even though we were not able to identify the pollen grains at the species level, we can assume that *Podocarpus* is associated with moist soil environments. Pollen grains of *Podocarpus* and *Araucaria* have low dispersal capacity (Ledru et al., 2007; Montade et al., 2019). Thus, we conclude that the almost unbroken record of their presence during the penultimate glacial implies development of trees in the vicinity of the core site and reflects humid climate conditions. Fluctuations in *Podocarpus* frequencies (0.3–18%) (Figure 3), more accentuated than for *Araucaria*, probably due to its larger size and its ability to feed on cloud drippings, were used to detect changes in moisture at the millennial scale. High Poaceae and Asteraceae frequencies together with tree taxa characteristic of high-elevation grassland, *Myrsine*, *Ilex* and *Symplocos* (Fig. S2) (Scheer & Micochinski, 2016; Portes et al., 2020), suggest a landscape of cold grassland with sparse conifers and low-standing tree species. The taxa associated with low temperatures (*Araucaria*, *Podocarpus*, *Acaena*, *Ephedra*) were not found in a modern pollen rain study of the high-elevation grassland of the State of Rio de Janeiro (Portes et al., 2020) where today's mean temperature is probably too high for their growth. Thus, we infer that, during the glacial epoch, changes in pollen frequencies of the above-mentioned indicators are related rather to moisture variability and seasonal distribution. In addition, *Podocarpus* pollen frequency and concentration follow the same variability (Fig. S3) showing that there was not an over-representation due to a local tree expansion and rather a regional-scale distribution (Birks & Birks, 1980).

Between 180 and 170 ka, fluctuations in the vegetation cover with four peaks of *Podocarpus* with high variability in both the pollen concentration and in the frequencies of AP were observed (Figure 3 and S3). The high incoherent/coherent ratio that relates to organic matter (see Rodríguez-Zorro et al., 2020) and the low silica content (Figure 3), for instance mica, which is abundant at the edge of the basin along with quartzites (Riccomini et al., 2011), suggest regular rainfall while the presence of the aquatic taxa *Isoetes* and *Botryococcus* suggest the presence of a shallow lake in the basin (Figure 3 and S2). This landscape is similar to the open landscape observed today above the upper forest limit with sparse *Podocarpus sellowii* in gallery forests, *Araucaria angustigolia* (Bertol.) Kuntze, and *P. lambertii* (Garcia & Pirani, 2005; Jeske-Pieruschka et al., 2010; Gonçalves et al., 2016), either in southern Brazil or restricted to high-elevation tropical grasslands, also called paramo-like grassland (Safford, 2001). The relatively low and continuous fire activity observed during this interval suggests remote seasonal burning (Leys et al., 2013) in agreement with the adaptation to burning of the plants that currently grow in the high-elevation grassland (Safford, 2001). Between ~167 and 160 ka, a sharp decrease in both conifer taxa *Araucaria* and *Podocarpus*, concomitant with the expansion of Poaceae and Asteraceae, suggest the development of a more open landscape than the one observed in the previous interval. The increase in Myrtaceae and Melastomataceae could represent either an artefact due to local humidity and the presence of a type of gallery forest around the lake or high-elevation species of these two genera, both of which are high pollen producers (Scheer & Mocochinski, 2016; Portes et al., 2020). Fire activity is still evident. Then, between ~155 and 140 ka, we observed a significant decrease in pollen concentration (Figure 2), the continuous presence of *Acaena* and a decrease in Moraceae/Urticaceae (Figure 3), which suggest drier and colder climatic conditions. The abrupt decrease in fire activity at ~148 ka also suggests changes in fuel properties (Safford, 2001). Peaks in fire activity are observed at 175 and 150 ka, during the low summer insolation phases, suggesting an open landscape with sparse trees of *P. sellowii* and frequent burning as observed today above the upper forest limit (Safford, 2001; Scheer and Mocochinski, 2016). Finally, between ~132 and 128 ka, a 2°C increase in temperature (Table 1) and overall lower fire activity are observed (Figure 3). *Podocarpus* frequencies are low (<3%) and, together with the presence of *Araucaria*, the regression of Poaceae and the expansion of Asteraceae suggest a significant change in the landscape in phase with the global increase in CO_2 (Shin et al., 2020). The decrease in the aquatic taxon *Myriophyllum* characterizes the progressive replacement of the lake by a bog (Fig. S2; Rodríguez-Zorro et al., 2020) in agreement with the changes in the lake predicted by diatoms (Figure 3 and S1). The penultimate glacial landscape at Colônia was composed of a grassland with conifers and probably small trees due to the low CO_2 (Shin et al., 2020) and low temperature. The continuous presence of austral conifers but with several oscillations suggest low temperature (MAAT 14.3°C) and a winter rainfall dominant regime different from the summer rainfall dominant regime we know today. Regression of the conifers occurred when the SASM became stronger preventing installation of winter rainfall (Rodríguez-Zorro et al., 2020). Today, high temperature and stronger SASM activity have induced a southward shift of the conifers (Ledru et al., 1994) which will probably become accentuated in the future (Wilson et al., 2021).

The penultimate glacial in the southern Tropics

MIS 6 is characterized by the development of a large ice sheet, extensive sea ice cover, low temperature in the South Atlantic, and relatively wet conditions with millennial-scale climate oscillations (Gottschalk et al., 2020). Sea level varied between −60 and −130, with an increase in sea level (–60 m) between 180 and 160 ka followed by a decrease to −140 m at 137 ka (Cawthra et al., 2018). In eastern Brazil (the western part of the South Atlantic), two marine records dating to the penultimate glacial (Figure 1b) reveal strong differences between the two last glacial stages (Santos et al., 2017; Hou et al., 2020). Moreover, reconstruction of the temperature gradient between the two sides of the South Atlantic showed that between 155 and 143 ka, a low E–W Atlantic SST gradient induced colder waters and lower

Table 1. Summary of the geochemical and charcoal results obtained for the studied interval (see Figure 2 for pollen zones) of core CO14 extracted from Rodríguez-Zorro et al. (2020).

Pollen zones	MAAT (°C, mean)	$\delta^{13}C$ (‰, mean)	Silica intensity	Charcoal particles (g^{-1})
C1 181–174 ka	14.2	−19.4695	2654	5642–222 326
C2 174–170 ka	14.2	−21.64	2662	27 928–396 558
C3 170–162 ka	14	−21.43	2686	149 852–44 465
C4 162–160 ka	14	−21.54	2930	138 332
C5 160–148 ka	14.5	−20.629	2873	330 234–60 249
C6 148–132 ka	14.5	−21.24	2512	315 260–11 008
C7 132–128 ka	15 at 132 ka 17 at 128 ka	−18.23	1212	177 860–22 024

SST offshore Brazil than during the glacial maximum (Hou et al., 2020). The closest marine record to Colônia, core GL-1090 (24.92°S, 42.51°W, 2225 m water depth) (Figures 1b and 4) (Santos et al., 2017) shows several oscillations of SSTs between 185 and 156 ka, from 24 to 27°C, with the lowest SSTs observed at 176, 172 and 160 ka. The lowest SST was observed between 156 and 153 ka and was followed by a progressive warming trend that reached 30°C at the beginning of the interglacial (Figure 4). After 140 ka, the beginning of the progressive warming trend observed in the South Atlantic is attributed to the increased influence of subtropical waters driven by the Agulhas leakage (Martínez-Méndez et al., 2010).

At Colônia, based on *Podocarpus* frequency (%) and concentration (Cn) (Fig. S3), we observed an out-of-phase relationship between austral summer (i.e. December–January–February) insolation and *Podocarpus* (Figure 4) with the near disappearance of *Podocarpus* during the austral summer insolation maximum phases observed at 180, 162 and 139 ka. As the expansion of *Podocarpus* requires humid conditions, we infer that low austral summer insolation is associated with high moisture rates at the latitude of Colônia during the penultimate glacial. Superimposed on this orbital trend, millennial-scale oscillations of *Podocarpus* lasting between 200 and 1000 years were observed between 180 and 170 ka and from 160 to ~143 ka (Figure 3 and S3).

The millennial-scale sawtooth pattern observed at Colônia looks similar to the instabilities observed in marine records, e.g. sedimentary molybdenum (Mo) at Cariaco (Gibson & Peterson, 2014), and ice records, e.g. methane and deuterium excess at Epica Dome C (EDC) (Loulergue et al., 2008) (Figure 4). Indeed, ice core methane events are usually linked to an increase in tropical wetlands associated with monsoon processes (Bock et al. 2017) while Antarctic ice deuterium and high moisture rates in the Tropics are interlinked in a feedback process (Vimeux et al., 2001). Between 180 and 160 ka high monsoon variability related to unstable conditions of the ITCZ during a low austral summer insolation phase was observed in the northern Tropics (Gibson & Peterson, 2014) and farther south in the high Peruvian Andes (Burns et al., 2019) (Figures 1a and 4). Thus, during early MIS 6, changes in moisture at Colônia followed the variability observed at both high (EDC; Jouzel et al., 2007) and low latitudes (Huagapo Cave; Burns et al., 2019), suggesting that the millennial-scale oscillations could be related to successive changes in the intensity and amplitude of the monsoon system and in the sea ice dynamics suggesting ice-volume forcing on the low-latitude hydrological cycle and on the floristic composition of the vegetation. Thus, we infer that penultimate glacial moisture oscillations at Colônia were controlled by the interplay between the position of the South Tropical Front (STF) (Pahnke & Zahn, 2005) and the ITCZ shifts which regulated the amplitude and intensity of the SASM. The conifer expansion suggests that the monsoon was not the dominant rainfall system, probably being restricted to a narrow band near the Equator and rarely reaching the latitude of Colônia. Dominant precipitations were brought by the northward shift of the STF enhancing winter rainfall at the latitude of Colônia (Grimm et al., 2000). Consequently, when the STF was shifted northward or southward from Colônia, drier conditions prevailed and induced a regression of the conifers as observed between ~167 and 160 ka. During this interval, the onset of drier conditions in the northern tropics (Tisserand et al., 2009) was linked to a southward shift of the ITCZ (Mulitza et al., 2008), in agreement with the more humid conditions observed at Huagapo (Burns et al., 2019) (Figure 4). However, the drier conditions observed at Colônia were not observed at EDC or at Huagapo, where the oscillations continued from the previous interval, suggesting that (i) the SASM system was positioned at the latitude of Huagapo but was unable to reach the latitude of Colônia due to a weaker amplitude and intensity than today, and (ii) changes in sea ice forcing and the position of the subtropical front prevented winter rains at Colônia.

The two other drier intervals at Colônia (low concentration of *Podocarpus*) are observed at 153–152 and 140–137 ka. The first low-*Podocarpus* event was associated with the lowest SST, the penultimate glacial maximum, observed in both the southwestern Atlantic (Santos et al., 2017) and the southwestern Pacific (Pahnke & Zahn, 2005) suggesting sea ice expansion. At Huagapo, this interval (158–152 ka) is characterized by weaker monsoon activity, in agreement with the Cariaco northward position of the ITCZ (Gibson & Peterson, 2014) while the northward shift of the STF observed in the southwestern Pacific (Pahnke et al., 2003) probably constrained precipitation further north of the latitude of Colônia. The second drier event at 140–137 ka occurred during a low sea level episode (Cawthra et al., 2018), a southwestern Pacific SST decrease and a northward shift of the STF (Pahnke & Zahn, 2005) while no change was observed in the SASM near the Equator (Burns et al., 2019) (Figure 4). TII started at ~145 ka at Colônia and was characterized by an increase in MAAT and in AP taxa, a decrease in cool conifer taxa and low erosive activity (low silica intensity) in the basin (Figure 2 and Table 1). The last *Podocarpus* and *Araucaria* expansion of the penultimate glacial, around 137–133 ka, coincides with a low austral summer insolation phase while the STF progressively shifted southward (Pahnke et al., 2003). This southward latitudinal shift in winter precipitation belts was observed at 42°S (New Zealand; Ryan et al., 2012) (Figure 1a) with TII starting at 140 ka, and characterized by a shift from an open environment to the expansion of the conifer *Podocarpus* during the continuous discharge of Antarctic ice between 140 and 131 ka (Masson-Delmotte et al., 2010). Climate reconstruction showed that meltwater release in the Southern Ocean induced a 2°C cooling at the latitude of Colônia (Swingedouw et al., 2009). Consequently, we infer that the joint effect of a strengthening monsoon and low temperature favored a short expansion of conifers during TII. The southern conifers declined after 133 ka, during the 135–130 ka Heinrich Stade 11, a cold episode induced by meltwater in the North Atlantic (Marino et al., 2015) with strong SASM response (Stríkis et al., 2018) and a progressive increase in temperature (Table 1).

The penultimate glacial high moisture rates observed at Colônia at an orbital scale resulted from a northward shift of the winter precipitation belt linked to Antarctic ice volume and the northward shift of the STF (Pahnke & Zahn, 2005) while millennial-scale shifts of the ITCZ controlled SASM intensity and amplitude across South America (Burns et al., 2019). The progressive disappearance of *Araucaria*, the development of a dry season, and the progressive dominance of the SASM system in the climate system that characterized the last glacial (MIS 2–4) (Rodríguez-Zorro et al., 2020) differed significantly from MIS 6. Due to the northernmost position of the ITCZ during MIS 6 (Reimi et al., 2019), the amplitude of the southern monsoon boundary never reached the latitude of Colônia and a dominant extratropical circulation is inferred to explain the floristic composition of the forest and its related hydrological cycle. Superimposed on this general feature, the Colônia record shows that climate change at the millennial scale has been a dominant feature of the tropical climate since at least the penultimate glacial. Indeed, a system that integrates sea ice expansion/regression in the Northern Hemisphere, latitudinal migration of the ITCZ and ice expansion in the Southern Hemisphere influenced the strength and amplitude of the monsoon system (Stríkis et al., 2018) and of the winter rainfall belt between the tropics and the sub-tropics (Ledru et al., 1994) relating to latitudinal shifts in rainforest boundaries that strongly influenced tropical forest biodiversity during the Quaternary.

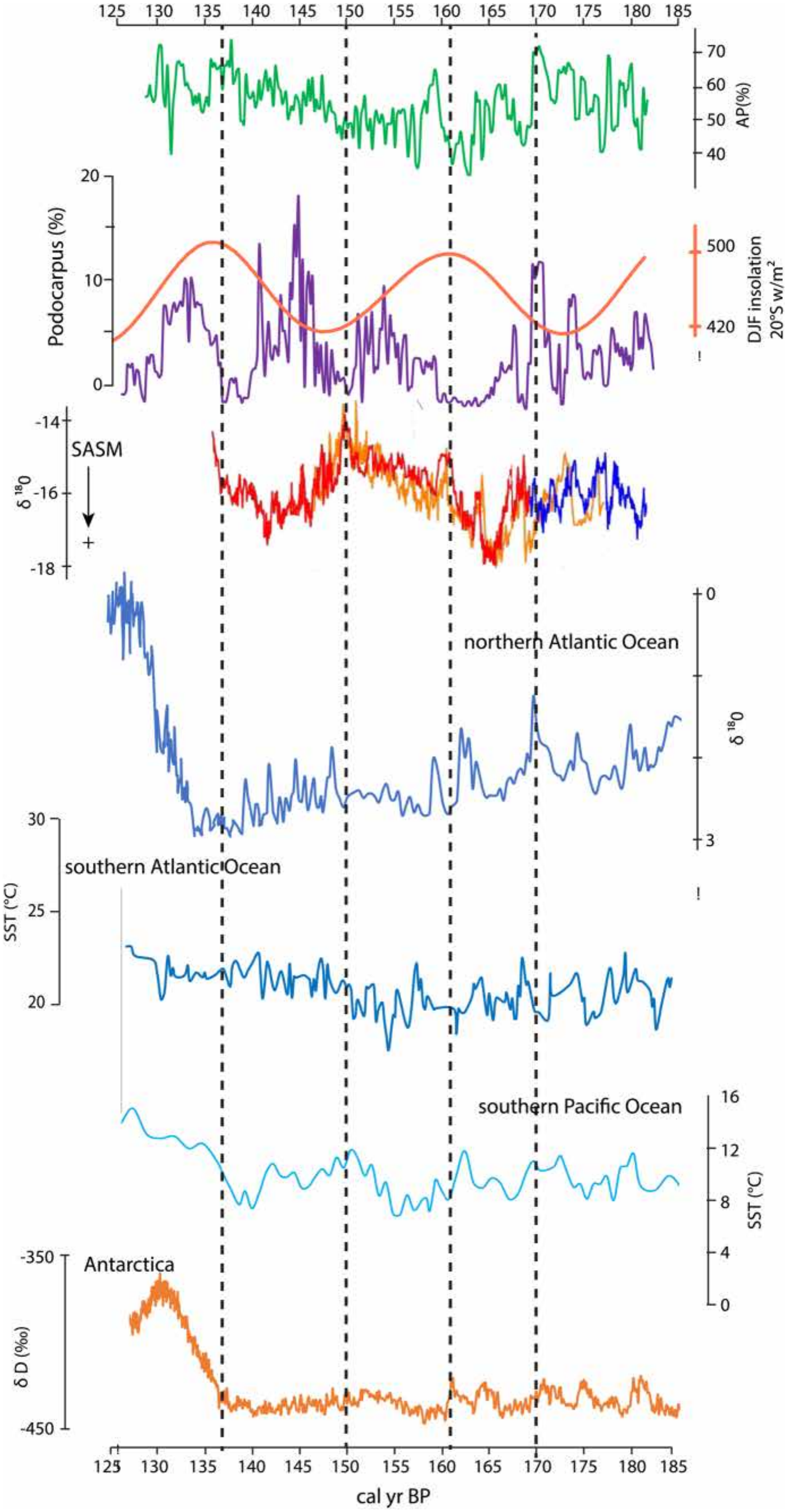

Figure 4. Regional comparison of the expression of MIS 6 between arboreal pollen and *Podocarpus* frequencies of Colônia (this study), changes in summer (DJF) insolation et 23°S latitude (Laskar et al., 2004), $\delta^{18}O$ of the speleothem of Huagapo (Burns et al., 2019) that characterizes SASM activity near the Equator, planktic $\delta^{18}O$ for SST (°C) of the Northern Atlantic Ocean (Hodell et al., 2023), *Globigerinoides ruber* $SST_{Mg/Ca}$ (°C) at the latitude of Colônia core GL-1090 (Santos et al., 2017), *Globigerina bulloides* $SST_{Mg/Ca}$ (°C) of the southwestern Pacific core (Pahnke & Zahn, 2005) that characterizes the volume of ice in the Southern Hemisphere and the shift in the STF, and deuterium (a temperature proxy) of the ice at EDC (Jouzel et al., 2007). The vertical dashed lines show the changes in vegetation discussed in the text. [Color figure can be viewed at wileyonlinelibrary.com]

Conclusion

The high-resolution pollen analyses of core CO14 collected from the Colônia basin have revealed an open landscape with cold forest taxa during the penultimate glacial and confirmed that fire is a long-term integral part of the ecology of cold tropical grasslands. The successive changes observed in the conifer *Podocarpus* were related to the reorganization of air masses between the Pole and the Equator in both hemispheres with changes in the boundary conditions of the SASM system through glacial–interglacial cycles. The penultimate glacial at the latitude of Colônia is characterized by a relatively high total AP frequency, with no change during the transition from glacial to interglacial, an orbitally driven variability with conifer expansion during low summer insolation phases and considerable variability at millennial timescales. Between around 170 and 160 ka, an interval that lasted ~10 ka showed no connection with other paleoclimatic records, thereby revealing specific climate behavior in the region of Colônia. During the penultimate glacial period, the climate at Colônia was characterized by a weaker influence of the monsoon and a lower MAAT than during the last glacial period. This pattern resulted from several forcings linked mainly to the positions of the STF and of the ITCZ. The combination of these factors strongly influenced Brazilian Atlantic forest biodiversity allowing the expansion of a paramo-like grassland at lower elevations than today with sparse tree components, many being the same Andean taxa. The expansion of high-elevation grassland to lowlands probably helped connect cold Andean and eastern Brazilian forest/grassland formations and taxa during this glacial stage of the Pleistocene.

Acknowledgements. This research is part of the project 'Dimensions of biodiversity' FAPESP (BIOTA 2013/50297-0), NSF (DEB 1343578) NASA, of the International Continental Deep Drilling Program (ICDP) and of the Labex-CEBA. A.M.C. acknowledges financial support from CAPES (001) and CNPQ (307333/2021-3). We thank Ulrich Struck for stable isotopes analyses at the Museum für Naturkunde, Berlin, Germany, and Rudney de Almeida Santos for improving some of the figures. G.C.M. thanks FAPESP (Fundação de Amparo à Pesquisa do Estado de São Paulo) for a Post-Doctoral fellowship (2018/10314-2) at the Instituto de Pesquisas Ambientais (INPA, São Paulo) linked to the project 'Challenges for biodiversity conservation' (FAPESP 2017/50341-0). The Area de Proteção Ambiental (APA) Capivari Monos, the association ACHAVE of the city of Vargem Grande are thanked for granting access to the drilling site and for their assistance during fieldwork.

Data availability statement

The data that support the findings of this study are available on request from the corresponding author. The data are not publicly available due to privacy or ethical restrictions.

Supporting information

Additional supporting information can be found in the online version of this article.

Figure S1. Summary diatom diagram showing changes in benthic and planktonic taxa. The absence of diatoms from 1125 cm corresponds to the transformation of the lake into a bog.

Figure S2. Full pollen diagram of section 870–1400 cm of core CO14.

Figure S3. Concentration and frequency of *Podocarpus* of section 870–1400 cm of core CO14.

Abbreviations. AP, arboreal pollen; H1 and H0, Heinrich event 1 and 0; ITCZ, Inter-Tropical Convergence Zone; MAAT, mean annual air temperature; MIS, Marine Isotopic Stage; NAP, non-arboreal pollen; SASM, South American Summer Monsoon; SST, sea surface temperature; STF, South Tropical Front; TII, Termination II.

References

Backes, A. (2009) Distribuição geográfica atual da Floresta com Araucária: condicionamento climático. In: Fonseca CR, Souza AF, Leal-Zanchet AM, Dutra TL, Backes A, Ganade G, editores. Floresta com Araucaria: Ecologia, Conservação e Desenvolvimento Sustentável. Ribeirão Preto: Editora Holos.

Battarbee, R.W. (1986) Diatom Analysis. In: Berglund, B.E., (ed.) *Handbook of Holocene Palaeoecology and Palaeohydrology*. Chichester: John Wiley & Sons Ltd. pp. 527–570.

Battarbee, R.W., Jones, V., Flower, R., Cameron, N.G., Bennion, H., Carvalho, L. et al. (2001) Diatoms. In: Smol, J.P., Birks, H.J.B., Last, W.M., (Eds.) *Tracking Enviromental Change Using Lake Sediments. Volume 3: Terrestrial, Algal, and Siliceous Indicators*. London: Kluwer Academic Publishers. pp. 155–203.

Bennett, K.D. (1996) Determination of the number of zones in a biostratigraphical sequence. *New Phytologist*, 132, 155–170. Available at: https://doi.org/10.1111/j.1469-8137.1996.tb04521.x

Bennett, K.D. (2009) *PSIMPOLL 4.27. Programs for Plotting Pollen Diagrams Analysing Pollen Data. 4.27*. Departament of Archaeology, Queens's University of Belfast, UK.

Bennett, S., Woods, T., Liyanage, W.M. & Smith, D.L. (1991) A Simplified general method for cluster-sample surveys of health in developing countries. *World health statistics quarterly. Rapport trimestriel de statistiques sanitaires mondiales*, 44, 98–106. https://apps.who.int/iris/handle/10665/47585

Bicudo, D.C., Tremarin, P.I., Almeida, P.D., Zorzal-Almeida, S., Wengrat, S., Faustino, S.B. et al. (2016) Ecology and distribution of *Aulacoseira* species (Bacillariophyta) in tropical reservoirs from Brazil. *Diatom Research*, 31, 199–215. Available at: https://doi.org/10.1080/0269249X.2016.1227376

Birks, H.J.B. & Birks, H.H. (1980) *The Quaternary palaeoecology*. University Park Press.

Bock, M., Schmitt, J., Beck, J., Seth, B., Chappellaz, J. & Fischer, H. (2017) Glacial/interglacial wetland, biomass burning, and geologic methane emissions constrained by dual stable isotopic CH4 ice core records. *Proceedings of the National Academy of Sciences*, 114, E5778–E5786. Available at: https://doi.org/10.1073/pnas.1613883114

Bogotá-A., R.G., Hooghiemstra, H. & Berrio, J.C. (2016) North Andean environmental and climatic change at orbital to submillennial timescales: vegetation, water-levels and sedimentary regimes from Lake Fúquene between 284 and 130ka. *Review of Palaeobotany and Palynology*, 226, 91–107. Available at: https://doi.org/10.1016/j.revpalbo.2015.09.007

Bradbury, J.P., Bezrukova, Y.V., Chernyaeva, G.P., Colman, S.M., Khursevich, G., King, J.W. et al. (1994) A synthesis of post-glacial diatom records from Lake Baikal. *Journal of Paleolimnology*, 10, 213–252.

Burns, S.J., Welsh, L.K., Scroxton, N., Cheng, H. & Edwards, R.L. (2019) Millennial and orbital scale variability of the South American monsoon during the penultimate glacial period. *Scientific Reports*, 9, 1234. Available at: https://doi.org/10.1038/s41598-018-37854-3

Caley, T., Giraudeau, J., Malaizé, B., Rossignol, L. & Pierre, C. (2012) Agulhas leakage as a key process in the modes of Quaternary climate changes. *Proceedings of the National Academy of Sciences*, 109, 6835–6839.

Camejo Aviles, A.M., Ledru, M.P., Ricardi-Branco, F., Rodríguez-Zorro, P.A., Francischetti Garcia, R.J. & Fernandez Perdomo, J. (2022) Characterization of a glacial neotropical rainforest from pollen and spore assemblages (Colônia, São Paulo, Brazil). *Grana*, 61, 81–123. Available at: https://doi.org/10.1080/00173134.2021.1976823

Cawthra, H.C., Jacobs, Z., Compton, J.S., Fisher, E.C., Karkanas, P. & Marean, C.W. (2018) Depositional and sea-level history from MIS 6 (Termination II) to MIS 3 on the southern continental shelf of South Africa. *Quaternary Science Reviews*, 181(1), 156–172. Available at: https://doi.org/10.1016/j.quascirev.2017.12.002

Colinvaux, P., De Oliveira, P.E. & Moreno, J.E. (1999) *Amazon pollen manual and atlas*. Amsterdam: Harwood Academic Publishers.

Costa, L.F., Wetzel, C.E., Lange-Bertalot, H., Ector, L. & Bicudo, D.C. (2017) Taxonomy and ecology of *Eunotia* species (Bacillariophyta) in southeastern Brazilian reservoirs. *Biblioth Diatomol*, 64, 1–302.

Cruz, F.W., Burns, S.J., Karmann, I., Sharp, W.D., Vuille, M., Cardoso, A.O. et al. (2005) Insolation-driven changes in atmospheric circulation over the past 116,000 years in subtropical Brazil. *Nature*, 434, 63–66. Available at: https://doi.org/10.1038/nature03365

DAEE. Departamento de águas e energia elétrica. (2020) Available in: http://www.hidrologia.daee.sp.gov.br/. (Acess jan. 23).

Davydova, N.N., Subetto, D.A., Khomutova, V.I. & Sapelko, T.V. (2001) Late Pleistocene-Holocene paleolimnology of three northwestern Russian lakes. *Journal of Paleolimnology*, 26, 37–51. Available at: https://doi.org/10.1023/A:1011131015322

DeForest Safford, H. (2007) Brazilian Páramos IV. Phytogeography of the campos de altitude. *Journal of Biogeography*, 34, 1701–1722. Available at: https://doi.org/10.1111/j.1365-2699.2007.01732.x

Faegri, K. & Iversen, J. (1989) *Textbook of Pollen Analysis*. Chichester: John Wiley & Sons.

Fernandez, J., Aviles, A.M.C., Ricardi-Branco, F.S.T., Ledru, M.P., Garcia, R.J.F. & Jurigan, I. (2021) Atlas palinológico atual da Bacia de Colônia, Estado de São Paulo, Brasil. *Terrae Didatica*, 17, e0210230. Available at: https://doi.org/10.20396/td.v17i00.8666074

Flora do Brasil. (2022) Jardim Botânico do Rio de Janeiro. http://floradobrasil.jbrj.gov.br/. Access 21 Dec. 2022

Fontana, L., Albuquerque, A.L.S., Brenner, M., Bonotto, D.M., Sabaris, T.P.P., Pires, M.A.F. et al. (2014) The eutrophication history of a tropical water supply reservoir in Brazil. *Journal of Paleolimnology*, 51, 29–43. Available at: https://doi.org/10.1007/s10933-013-9753-3

Garcia, R.J.F., Honda, S. & Fries, B.G. (2014) Estudo florístico de segmento de mata atlântica em Parelheiros, São Paulo, SP, para soltura de bugio-ruivo, *Alouatta clamitans* (Cabrera, 1940). *Revista do Instituto Florestal*, 26, 71–87. https://doi.org/10.4322/rif.2014.005

Garcia, R.J.F. & Pirani, J.R. (2003) Revisão sobre o diagnostico e caracterização da vegetação campestre junto a cista de serras, no Parque Estadual das Serra do Mar, São Paulo, Brasil. *Hoehnea*, 30, 217–242.

Garcia, R.J.F. & Pirani, J.R. (2005) Análise florística, ecológica e fitogeográfica do Núcleo Curucutu, Parque Estadual da Serra do Mar (São Paulo, SP), com ênfase nos campos junto à crista da Serra do mar. *Hoehnea*, 32, 1–48.

Gell, P.A., Barker, P.A., De Deckker, P., Last, W.M. & Jelicic, L. (1994) The Holocene history of West Basin Lake Victoria, Australia: chemical changes based on fossil biota and sediment mineralogy. *Journal of Paleolimnology*, 12, 235–258.

Gibson, K.A. & Peterson, L.C. (2014) A 0.6-million-year record of millennial-scale climate variability in the tropics. *Geophysical Research Letters*, 41, 969–975. Available at: https://doi.org/10.1002/2013GL058846

Gonçalves, F.R., Vieira, F.A. & Carvalho, D. (2016) Naturally fragmented but not genetically isolated populations of *Podocarpus sellowii* Klotzsch (Podocarpaceae) in southeast Brazil. *Genetics and Molecular Research*, 15, gmr8871. Available at: https://doi.org/10.4238/gmr.15048871

Gottschalk, J., Skinner, L.C., Jaccard, S.L., Menviel, L., Nehrbass-Ahles, C. & Waelbroeck, C. (2020) Southern Ocean link between changes in atmospheric CO_2 levels and northern-hemisphere climate anomalies during the last two glacial periods. *Quaternary Science Reviews*, 230, 106067. Available at: https://doi.org/10.1016/j.quascirev.2019.106067

Grimm, A.M., Barros, V.R. & Doyle, M.E. (2000) Climate variability inSouthern South America associated with El Niño and La Niñaevents. *Journal of Climate*, 13, 35–58. Available at: https://doi.org/10.1175/1520-0442(2000)

Guarinello de Oliveira Portes, M.C., DeForest Safford, H., Montade, V. & Behling, H. (2020) Pollen rain–vegetation relationship along an elevational gradient in the Serra dos Órgãos National Park, southeastern Brazil. *Review of Palaeobotany and Palynology*, 283, 104314. Available at: https://doi.org/10.1016/j.revpalbo.2020.104314

Hanselman, J.A., Bush, M.B., Gosling, W.D., Collins, A., Knox, C., Baker, P.A. et al. (2011) A 370,000-year record of vegetation and fire history around Lake Titicaca (Bolivia/Peru). *Palaeogeography, Palaeoclimatology, Palaeoecology*, 305, 201–214. Available at: https://doi.org/10.1016/j.palaeo.2011.03.002

Hargan, K.E., Rühland, K.M., Paterson, A.M., Finkelstein, S.A., Holmquist, J.R., MacDonald, G.M. et al. (2015) The influence of water-table depth and pH on the spatial distribution of diatom species in peatlands of the Boreal Shield and Hudson Plains, Canada. *Botany*, 93, 57–74. Available at: https://doi.org/10.1139/cjb-2014-0138

Hodell, D.A., Crowhurst, S.J., Lourens, L., Margari, V., Nicolson, J., Rolfe, J.E. et al. (2023) A 1.5-million-year record of orbital and millennial climate variability in the North Atlantic. *Climate of the Past*, 19, 607–636. Available at: https://doi.org/10.5194/cp-19-607-2023

Hou, A., Bahr, A., Schmidt, S., Strebl, C., Albuquerque, A.L., Chiessi, C.M. et al. (2020) Forcing of western tropical South Atlantic sea surface temperature across three glacial-interglacial cycles. *Global and Planetary Change*, 188, 103150. Available at: https://doi.org/10.1016/j.gloplacha.2020.103150

INMET- Instituto Nacional de Meteorologia. (2019) Available at: https://www.gov.br/agricultura/pt-br/assuntos/inmet. Accessed January 2022.

Jeske-Pieruschka, V., Fidelis, A., Bergamin, R.S., Vélez, E. & Behling, H. (2010) Araucaria forest dynamics in relation to fire frequency in southern Brazil based on fossil and modern pollen data. *Review of Palaeobotany and Palynology*, 160, 53–65. Available at: https://doi.org/10.1016/j.revpalbo.2010.01.005

Jouzel, J., Masson-Delmotte, V., Cattani, O., Dreyfus, G., Falourd, S., Hoffmann, G. et al. (2007) Orbital and Millennial Antarctic Climate Variability over the Past 800,000 Years. *Science*, 317, 793–796. Available at: https://doi.org/10.1126/science.1141038

Juggins, S. (2017) Rioja: analysis of quaternary science data, R package version. Available at: http://cran.r-project.org/package=rioja.0.9-21

Kern, A.K., Akabane, T.K., Ferreira, J.Q., Chiessi, C.M., Willard, D.A., Ferreira, F. et al. (2023) A 1.8 million year history of Amazon vegetation. *Quaternary Science Reviews*, 299, 107867. Available at: https://doi.org/10.1016/j.quascirev.2022.107867

Kershaw, A.P., Bretherton, S.C. & van der Kaars, S. (2007) A complete pollen record of the last 230 ka from Lynch's Crater, north-eastern Australia. *Palaeogeography, Palaeoclimatology, Palaeoecology*, 251, 23–45. Available at: https://doi.org/10.1016/j.palaeo.2007.02.015

Kessler, M. (1955) The genus *Polylepis* (Rosaceae) in Bolivia. *Candollea*, 42, 31–71.

Komárek, J. & Jankovská, V. (2001) Review of the green algal genus *Pediastrum*; implication for pollen analytical research. *Bibl Phycol*, 108, 1–127.

Krammer, K. (2000) The genus *Pinnularia*. In: Lange-Bertalot, H., (ed.) *Diatoms of Europe. Diatoms of the European Inland waters and comparable habitats*. Ruggell: ARG Gantner Verlag KG. p. 703.

Lamy, F., Gersonde, R., Winckler, G., Esper, O., Jaeschke, A., Kuhn, G. et al. (2014) Increased Dust Deposition in the Pacific Southern Ocean During Glacial Periods. *Science*, 343, 403–407. Available at: https://doi.org/10.1126/science.1245424

Laskar, J., Robutel, P., Joutel, F. Gastineau, M., Correia, A.C.M. & Levrard, B. (2004) A long term numerical solution for the insolation quantities of the Earth. Astronomy & Astrophysics, 428, 261-285. https://doi.org/10.1051/0004-6361:20041335

Leal, A., Berrío, J.C., Raimúndez, E. & Bilbao, B. (2011) A pollen atlas of premontane woody and herbaceous communities from the upland savannas of Guayana, Venezuela. *Palynology*, 35, 226–266. Available at: https://doi.org/10.1080/01916122.2011.603909

Ledru, M.-P., Behling, H., Fournier, M., Martin, L. & Servant, M. (1994) Position of the Brazilian *Araucaria* forest during the Holocene. Paleoclimatic implications. *Comptes Rendus de l'Académie des Sciences de Paris*, 317, 517–521.

Ledru, M.P., Mourguiart, P., Ceccantini, G., Turcq, B. & Sifeddine, A. (2002) Tropical climates in the game of two hemispheres revealed by abrupt climatic change. *Geology*, 30, 275–278.

Ledru, M.P., Mourguiart, P. & Riccomini, C. (2009) Related changes in biodiversity, insolation, and climate in the Atlantic rainforest since the last interglacial. *Palaeogeography, Palaeoclimatology, Palaeoecology*, 271, 140–152. Available at: https://doi.org/10.1016/j.palaeo.2008.10.008

Ledru, M.P., Reimold, W.U., Ariztegui, D., Bard, E., Crósta, A.P., Riccomini, C. et al. (2015) Why deep drilling in the Colônia Basin (Brazil)? *Scientific Drilling*, 20, 33–39. Available at: https://doi.org/10.5194/sd-20-33-2015

Ledru, M.P., Salatino, M.L.F., Ceccantini, G., Salatino, A., Pinheiro, F. & Pintaud, J.C. (2007) Regional assessment of the impact of climatic change on the distribution of a tropical conifer in the lowlands of South America. *Diversity and Distributions*, 13, 761–771. Available at: https://doi.org/10.1111/j.1472-4642.2007.00389.x

Leys, B., Carcaillet, C., Dezileau, L., Ali, A.A. & Bradshaw, R.H.W. (2013) A comparison of charcoal measurements for reconstruction of Mediterranean paleo-fire frequency in the mountains of Corsica. *Quaternary Research*, 79, 337–349. http://dx.doi.org/10.1016/j.yqres.2013.01.003

Lorente, F., Buso, A., De Oliveira, P.E. & Pessenda, L.C.R. (2017) Palynological Atlas. 14C Laboratory-CENA/USP. FEALQ, Piracicaba, São Paulo.

Lorscheitter, M.L., Ashraf, A., Bueno, R. & Mosburger, V. (1998) Pteridophyte spores of Rio Grande do Sul flora. *Brazil. Part I. Palaeontographica*, 246, 1–113.

Lorscheitter, M.L., Ashraf, A., Windisch, P. & Mosburger, V. (1999) Pteridophyte spores of Rio Grande do Sul flora. *Brazil. Part II. Palaeontographica*, 251, 71–235.

Loulergue, L., Schilt, A., Spahni, R., Masson-Delmotte, V., Blunier, T., Lemieux, B. et al. (2008) Orbital and millennial-scale features of atmospheric CH4 over the past 800,000 years. *Nature*, 453, 383–386. Available at: https://doi.org/10.1038/nature06950

Mackay, A.W., Ryves, D.B., Battarbee, R.W., Flower, R.J., Jewson, D., Rioual, P. et al. (2005) 1000 years of climate variability in central Asia: assessing the evidence using Lake Baikal (Russia) diatom assemblages and the application of a diatom-inferred model of snow cover on the lake. *Global and Planetary Change*, 46, 281–297. Available at: https://doi.org/10.1016/j.gloplacha.2004.09.02

Marchant, R., Almeida, L., Behling, H., Berrio, J.C., Bush, M., Cleef, A. et al. (2002) Distribution and ecology of parent taxa of pollen lodged within the Latin American Pollen Database. *Review of Palaeobotany and Palynology*, 121, 1–75. Available at: https://doi.org/10.1016/S0034-6667(02)00082-9

Marçon, S.L. (2009) Composição florística e estrutura do componente arbustivo-arbóreo do Parque Natural Municipal da Cratera de Colônia, São Paulo, SP. Dissertation (Master in Comparative Biology) - Faculty of Biology, University of São Paulo.

Marengo, J.A., Ambrizzi, T., Alves, L.M., Barreto, N.J.C., Simões Reboita, M. & Ramos, A.M. (2020) Changing Trends in Rainfall Extremes in the Metropolitan Area of São Paulo: Causes and Impacts. *Frontiers in Climate*, 2, 2624–9553. Available at: https://doi.org/10.3389/fclim.2020.0000

Marino, G., Rohling, E.J., Rodríguez-Sanz, L., Grant, K.M., Heslop, D., Roberts, A.P. et al. (2015) Bipolar seesaw control on last interglacial sea levelBipolar seesaw control on last interglacial sea level. *Nature*, 522, 197–201.

Markgraf, V. (ed.) (2001) *Interhemispheric Climate Linkages*. Elsevier. p. 454

Marquardt, G.C., Bicudo, D.C., Bicudo, C.E., Ledru, M.-P., Ector, L. et al. (2021a) *Pseudostaurosira crateri* sp. nov. (Fragilariaceae, Bacillariophyta), a new fossil small-araphid diatom species from the Pleistocene (Brazilian Coastal Plain, Atlantic Forest, São Paulo Metropolitan Region). *Phytotaxa*, 496, 105–120. Available at: https://doi.org/10.11646/phytotaxa.496.2.1

Marquardt, G.C., Bicudo, D.C., Bicudo, C.E., Ledru, M.-P., Ector, L. & Wetzel, C. (2021b) *Planothidium scrobiculatum* sp. nov. (Bacillariophyta), a new monoraphid diatom from freshwater Pleistocene deposits of South America. *Fottea*, 21, 53–61. Available at: https://doi.org/10.5507/fot.2020.016

Martínez-Garcia, A., Rosell-Melé, A., McClymont, E.L., Gersonde, R. & Haug, G.H. (2010) Subpolar Link to the emergence of the modern equatorial Pacific Cold Tongue. *Science*, 328, 1550–1553. Available at: https://doi.org/10.1126/Science

Martínez-Méndez, G., Zahn, R., Hall, I.R., Peeters, F.J.C., Pena, L.D., Cacho, I. et al. (2010) Contrasting multiproxy reconstructions of surface ocean hydrography in the Agulhas Corridor and implications for the Agulhas Leakage during the last 345,000 years. *Paleoceanography and Paleoclimatology*, 25, PA4227. Available at: https://doi.org/10.1029/2009PA001879

Masson-Delmotte, V., Stenni, B., Blunier, T., Cattani, O., Chappellaz, J., Cheng, H. et al. (2010) Abrupt change of Antarctic moisture origin at the end of Termination II. *Proceedings of the National Academy of Sciences*, 107, 12091–12094. Available at: https://doi.org/10.1073/pnas.0914536107

Metzeltin, D. & Lange-Bertalot, H. (1998) Tropical diatoms of South America. *Iconogr Diatomol*, 5, 1–695.

Montade, V., Ledru, M.P., Giesecke, T., Flantua, S.G., Behling, H. & Peyron, O. (2019) A new modern pollen dataset describing the Brazilian Atlantic Forest. *The Holocene*, 29, 1253–1262. Available at: https://doi.org/10.1177/0959683619846981

Mulitza, S., Prange, M., Stuut, J.-B., Zabel, M., Debeneck, T., Itambi, A.C. et al. (2008) Sahel megadroughts triggered by glacial slowdowns of Atlantic meridional overturning. *Paleoceanography and Paleoclimatology*, 23, PA420 6. Available at: https://doi.org/10.1029/2008PA001637

Obrochta, S.P., Crowley, T.J., Channell, J.E.T., Hodell, D.A., Baker, P.A., Seki, A. et al. (2014) Climate variability and ice-sheet dynamics during the last three glaciations. *Earth and Planetary Science Letters*, 406, 198–212. Available at: https://doi.org/10.1016/j.epsl.2014.09.004

Oksanen, J., Blanchet, F.G., Friendly, M.H., Kindt, R., Legendre, P., McGlinn, D. et al. (2019) Vegan: community ecology package. The R Project for Statistical Computing. http://CRAN.R

Orrison, R., Vuille, M., Smerdon, J.E., Apaéstegui, J., Azevedo, V., Campos, J.L.P.S. et al. (2022) South American Summer Monsoon variability over the last millennium in paleoclimate records and isotope-enabled climate models. *Climate of the Past*, 18, 2045–2062. Available at: https://doi.org/10.5194/cp-18-2045-2022

Pahnke, K. & Zahn, R. (2005) Southern Hemisphere water mass conversion linked with North Atlantic climate variability. *Science* 307: 1741-1746. Available at: https://doi.org/10.1126/science.1102163

Pahnke, K., Zahn, R., Elderfield, H. & Schulz, M. (2003) 340,000-year centennial-scale marine record of Southern Hemisphere climatic oscillation. *Science*, 301, 948–952. Available at: https://doi.org/10.1126/science.1084451

Palaeosens Project Members (2012) Making sense of palaeoclimate sensitivity. *Nature*, 491, 683–691. Available at: https://doi.org/10.1038/nature11574

Pappas, J.L. & Stoermer, E.F. (1996) Quantitative method for determining a representative algal sample count. *Journal of Phycology*, 32, 693–696. Available at: https://doi.org/10.1111/j.0022-3646.1996.00693.x

Paull, T.M., Finkelstein, S.A. & Gajewski, K. (2017) Interactions between climate and landscape drive Holocene ecological change in a High Arctic lake on Somerset Island, Nunavut, Canada. *Arctic Science*, 3, 17–38. Available at: https://doi.org/10.1139/as-2016-0013

Prado, R.L., Espin Fenoll, I.C., Ullah, I., Miura, G.C.M., Crósta, A.P., Zanon dos Santos, R.P. et al. (2019) Geophysical investigation of the Colônia structure, Brazil. *Meteoritics & Planetary Science*, 54, 2357–2372. Available at: https://doi.org/10.1111/maps.13292

Quiroga, M.P., Mathiasen, P., Iglesias, A., Mill, R.R. & Premoli, A.C. (2016) Molecular and fossil evidence disentangle the biogeographical history of Podocarpus, a key genus in plant geography. *Journal of Biogeography*, 43, 372–383. Available at: https://doi.org/10.1111/jbi.12630

R Core Team. (2022) *R: A language and environment for statistical computing, version 4.2. 2*. R Foundation for Statistical Computers, Vienna.

Reimi, M.A., Marcantonio, F., Lynch-Stieglitz, J., Jacobel, A.W., McManus, J.F. & Winckler, G. (2019) The Penultimate Glacial Termination and Variability of the Pacific Intertropical Convergence Zone. *Geophysical Research Letters*, 46, 4826–4835. Available at: https://doi.org/10.1029/2018GL081403

Riccomini, C., Crósta, A.P., Prado, R.L., Ledru, M.P., Turcq, B., Sant'Anna, L.G. et al. (2011) The Colônia structure, São Paulo, Brazil. *Meteoritics & Planetary Science*, 46, 1630–1639. Available at: https://doi.org/10.1111/j.1945-5100.2011.01252.x

Riccomini, C., Turcq, B., Martin, L., Moreira, M.Z. & Lorscheitter, M.L. (1991) The Colônia astrobleme, Brasil. *Revista do Instituto Geológico*, 12, 87–94. Available at: https://doi.org/10.5935/0100-929X.19910007

Rodbell, D.T., Hatfield, R.G., Abbott, M.B., Chen, C.Y., Woods, A., Stoner, J.S. et al. (2022) 700,000 years of tropical Andean glaciation. *Nature*, 607, 301–306. Available at: https://doi.org/10.1038/s41586-022-04873-0

Rodríguez-Zorro, P.A., Ledru, M.-P., Bard E., Aquino-Alfonso, O., Camejo Aviles, A.M., Daniau, A.-L. et al. (2020) Shutdown of the South American summer monsoon during the penultimate glacial. *Nature Scientific Reports*, 10, 6275. Available from: https://doi.org/10.1038/s41598-020-62888-x

Rühland, K., Jacques, J.-M.S., Beierle, B.D., Lamoureux, S.F., Dyke, A.S. & Smol, J.P. (2009) Lateglacial and Holocene paleoenvironmental changes recorded in lake sediments, Brock Plateau (Melville Hills), Northwest Territories, Canada. *The Holocene*, 19, 1005–1016. Available at: https://doi.org/10.1177/0959683609340999

Ryan, M.T., Dunbar, G.B., Vandergoes, M.J., Neil, H.L., Hannah, M.J., Newnham, R.M. et al. (2012) Vegetation and climate in Southern Hemisphere mid-latitudes since 210 ka: new insights from marine and terrestrial pollen records from New Zealand. *Quaternary Science Reviews*, 48, 80–98. Available at: https://doi.org/10.1016/j.quascirev.2012.06.001

Safford, H.D. (2001) Brazilian Páramos. III. Patterns and Rates of Postfire Regeneration in the Campos de Altitude. *Biotropica*, 33, 282–302. Available at: https://doi.org/10.1111/j.1744-7429.2001.tb00179.x

Salgado-Labouriau, M.L. (1979) Modern pollen deposition in the Venezuelan Andes. *Grana*, 18, 53–68. Available at: https://doi.org/10.1080/00173137909428871

Santos, T.P., Lessa, D.O., Venancio, I.M., Chiessi, C.M., Mulitza, S., Kuhnert, H. et al. (2017) Prolonged warming of the Brazil Current precedes deglaciations. *Earth and Planetary Science Letters*, 463, 1–12. Available at: https://doi.org/10.1016/j.epsl.2017.01.014

Scheer, M.B. & Mocochinski, A.Y. (2016) Upper montane grassland structure within six subranges of Serra do Mar, Southern Brazil. *Hoehnea*, 43, 401–435.

Schneider, T., Bischoff, T. & Haug, G.H. (2014) Migrations and dynamics of the intertropical convergence zone. *Nature*, 513, 45–53. Available at: https://doi.org/10.1038/nature13636

Shin, Y., Lee, Y. & Park, J.S. (2020) A weighting scheme in a multi-model ensemble for bias-corrected climate simulation. *Atmosphere*, 11, 775.

Shulmeister, J., Rodbell, D.T., Gagan, M.K. & Seltzer, G.O. (2006) Inter-hemispheric linkages in climate change: paleo-perspectives for future climate. *Climate of the Past*, 2, 167–185. Available at: https://doi.org/10.5194/cp-2-167-2006

Simon, Q., Ledru, M.P., Sawakuchi, A.O., Favier, C., Mineli, T.D., Grohmann, C.H. et al. (2020) Chronostratigraphy of a 1.5 ± 0.1 Ma composite sedimentary record from Colônia basin (SE Brazil): Bayesian modeling based on paleomagnetic, authigenic 10Be/9Be, radiocarbon and luminescence dating. *Quaternary Geochronology*, 58, 101081. Available at: https://doi.org/10.1016/j.quageo.2020.101081

Sterken, M., Verleyen, E., Sabbe, K., Terryn, G., Charlet, F., Bertrand, S. et al. (2008) Late Quaternary climatic changes in southern Chile, as recorded in a diatom sequence of Lago Puyehue (40°40'S). *Journal of Paleolimnology*, 39, 219–235. Available at: https://doi.org/10.1007/s10933-007-9114-1

Stríkis, N.M., Cruz, F.W., Barreto, E.A.S., Naughton, F., Vuille, M., Cheng, H. et al. (2018) South American monsoon response to iceberg discharge in the North Atlantic. *Proceedings of the National Academy of Sciences*, 115, 3788–3793. Available at: https://doi.org/10.1073/pnas.1717784115

Swingedouw, D., Fichefet, T., Goosse, H. & Loutre, M.F. (2009) Impact of transient freshwater releases in the Southern Ocean on the AMOC and climate. *Climate Dynamics*, 33, 365–381.

Teixeira, A.P. & Assis, M.A. (2011) Floristic relationships among inland swamp forests of Southeastern and Central-Western Brazil. *Revista Brasileira de Botânica*, 34, 91–101. Available at: https://doi.org/10.1590/S0100-84042011000100009

Tisserand, A., Malaizé, B., Jullien, E., Zaragosi, S., Charlier, K. & Grousset, F. (2009) African monsoon enhancement during the penultimate glacial period (MIS 6.5 - 170 ka) and its atmospheric impact. *Paleoceanography and Paleoclimatology*, 24, PA2220. Available at: https://doi.org/10.1029/2008PA001630

Torres, V., Hooghiemstra, H., Lourens, L. & Tzedakis, P.C. (2013) Astronomical tuning of long pollen records reveals the dynamic history of montane biomes and lake levels in the tropical high Andes during the Quaternary. *Quaternary Science Reviews*, 63, 59–72. Available at: https://doi.org/10.1016/j.quascirev.2012.11.004

Tremarin, P.I., Ludwig, T.V. & Torgan, L.C. (2013) Morphological variation and distribution of the freshwater diatom *Aulacoseira ambigua* (Grunow) Simonsen in Brazilian continental environments. *Iheringia*, 68, 139–157.

Tyson, R.V. (1995) Abundance of Organic Matter in Sediments: TOC, Hydrodynamic Equivalence, Dilution and Flux Effects. In: Tyson, R.V., (ed.) *Sedimentary Organic Matter*. Dordrecht: Springer. pp. 81–118. https://doi.org/10.1007/978-94-011-0739-6_5

Unkel, I., Fernandez, M., Björck, S., Ljung, K. & Wohlfarth, B. (2010) Records of environmental changes during the Holocene from Isla de los Estados (54.4°S), southeastern Tierra del Fuego. *Global and Planetary Change*, 74, 99–113.

Vimeux, F., Masson, V., Delaygue, G., Jouzel, J., Petit, J.R. & Stievenard, M. (2001) A 420,000-year deuterium excess record from East Antarctica: Information on past changes in the origin of precipitation at Vostok. *Journal of Geophysical Research: Atmospheres*, 106, 31863–31873.

Wilson, O.J., Mayle, F.E., Walters, R.J., Lingner, D.V. & Vibrans, A.C. (2021) Floristic change in Brazil's Southern Atlantic forest biodiversity hotspot: From the last glacial maximum to the late 21st century. *Quaternary Science Reviews* 264, 107005. https://doi.org/10.1016/j.quascirev.2021.107005

World Ocean Atlas. (2018) Available at: https://www.ncei.noaa.gov/access/world-ocean-atlas-2018/

Zheng, Z., Huang, K., Deng, Y., Cao, L., Yu, S., Suc, J.P. et al. (2013) A ~200 ka pollen record from Okinawa Trough: Paleoenvironment reconstruction of glacial-interglacial cycles. *Science China Earth Sciences*, 56, 1731–1747. Available at: https://doi.org/10.1007/s11430-013-4619-0